# Basicity of Urea: Near-Infrared Spectroscopic and Theoretical Studies on the Hydrogen Bonding Ability of TMU and DMDPU

**Ho-Jin Lee, Jeunghee Park†, Chang-Ju Yoon‡, and Young Sang Choi***

*Department of Chemistry, Korea University, Seoul 136-701, Korea*
*†Department of Chemistry, Korea University, Jochiwon 339-700, Korea*
*‡Department of Chemistry, Catholic University, Bucheon 422-743, Korea*
*Received October 9, 1997*

The hydrogen-bonding interactions between thioacetamide (TA) and urea derivatives such as tetramethylurea (TMU) and dimethyldiphenylurea (DMDPU) have been studied using near-infrared absorption spectroscopy. Thermodynamic parameters for the interactions between TA and urea derivatives were determined by analyzing the $\nu_{N,H}^{as}$+Amide II combination band of TA at 1970 nm. The $\Delta H^{\circ}$ values, indicating the intrinsic strength of hydrogen bonding, are −23.0 kJ/mol and −19.8 kJ/mol for TMU and DMDPU, respectively. This is well explained by the inductive effects of substituents. *Ab initio* molecular orbital calculations for the proton affinity of TMU, *N,N*-dimethylformamide (DMF), and *N,N*-dimethylacetamide (DMA) in gas phase have been carried out at HF/3-21G ad HF/6-31G(d) levels, showing that the proton affinity of TMU is larger than that of DMA, which agrees with the experimental results.

## Introduction

Aqueous urea solution has been extensively investigated experimentally, but also theoretically by molecular simulations. Urea is highly soluble in water;[1] it increases the solubility of hydrocarbons in water[2] and denaturates proteins.[3] These properties have been rationalized with different, mutually exclusive several models of the hydration.[4,5] One of the models is the indirect mechanism where urea alters the ordinary pure water structure in the vicinity of solutes.[4] The urea acts as a breaker of water structure. Another mechanism is the direct mechanism;[5] the hydrocarbons are solvated by both urea and water molecules and the formation of urea dimers and oligomers is central.

Urea-water mixtures have also been studied in several molecular simulations.[6-9] Kuharski and Rossky argue strongly against the role of urea as a water structure breaker.[6] In a simulation of urea and an apolar solute in water, the authors find that direct interaction between urea and the apolar solute dominates over the indirect solvent reorganization energy. This supports the direct mechanism, where hydrocarbons are solvated by both urea and water molecules. Tanaka *et al.* also found that one urea and water molecule could be solvated by both urea and water molecules without distorting the water structures and the tightly bound urea dimers become important with increasing concentration.[7] However, Cristinziano et al. found the dimer to be unstable in solution and argued a solvent separation of the urea dimer by calculating the energetics of urea dimers in water clusters.[8] Finney and Turner have pointed out an inconsistency in the structure of urea solutions between simulations and neutron scattering experiments.[9] The simulation fails to reproduce the oscillatory behavior and the location of the maximum in the total nitrogen radial distribution function.

The effect of urea derivatives, *e.g.* tetramethylurea (TMU), on the water structure has also been the subject of contrasting opinions. TMU is one of the few urea derivatives that are liquid at room temperature, and is miscible in all proportion with water. Barone *et al.* report that TMU and other urea derivatives act as water structuring agents, while the urea acts as a water-breaking agent.[10] However, Subramanian *et al.* used the chemical shift of $^1$H NMR, suggesting that dimethylurea and TMU in aqueous solution show the structure making behavior until the concentration of TMU is reached to 2 M, but becomes structure-breaking at higher concentration than 2 M.[11] More recently, Jancsó *et al.* employed small-angle neutron scattering (SANS) technique to study the hydrophobic interaction in aqueous TMU solution, suggesting that the structure of water is altered until the volume fraction ratio of TMU to water is 0.07.[12] Therefore, in spite of numerous works, the exact mechanism for the protein denaturation process of urea and its derivatives in water still remains to be elucidated.

In this work, we try to understand the hydrogen bonding effect of urea on denaturation of protein. Thioacetamide (TA) is selected as a simple protein mimic model and the hydrogen bonding ability of TMU with TA in $CCl_4$ solution has been investigated using near-infrared spectroscopic technique. The hydrogen bonding ability of urea is examined by using dimethyldiphenylurea (DMDPU). The proton affinity (PA), a measurement of its basicity, is defined as the enthalpy change at 298.15 K for the protonation process. The enthalpy change for $TMU(g)+H^+(g) \rightarrow TMUH^+(g)$, PA of TMU, is an important parameter for understanding the fundamental nature of hydrogen bonding interaction. The structural data as well as the proton affinity have been calculated to analyze what factors affect the basicity of TMU toward the hydrogen bonding. We also carry out *ab initio* calculation for the amides such as *N,N*-dimethylacetamide (DMA) and *N,N*-dimethyformamide (DMF) in order to consider the effect of substituent on the molecular properties.

*To whom correspondence should be addressed.

## Experimental

TA (Riedel-deHaen, 99%) was dried at room temperature under reduced pressure for 24 hours and used without further purification. TMU (Aldrich, 99%) and $CCl_4$ (Barker, HPLC grade) were dried over 4 Å molecular sieves. The mole ratio of TMU and DMDPU to TA is 1:6 and 1:5, respectively, in CCl4 to measure the equilibrium constants for the formation of 1:1 complex in the temperature range of 5-45 °C.

The near-IR absorption spectra of TA were obtained with Cary 17D spectrophotometer (Varian Co.), using 10 cm path length cylindrical quartz cell. The bands due to TMU and solvent were eliminated by placing a matching cell containing equal amounts of proton acceptor in the path of the reference beam. The sample and reference cells were placed in a jacketed cell-holder connected to a constant temperature bath. The temperature fluctuation during the measurement was less than ±0.2 °C.

All calculations have been performed using Gaussian 94 W program.

## Results and Discussion

**Near-infrared spectroscopic studies on the hydrogen bonding ability of TMU and DMDPU.** In order to study the hydrogen bonding of TA with urea derivatives in $CCl_4$, the near infrared absorption spectroscopic technique has been employed. The combination band of antisymmetric N-H stretching ($\nu_{N\text{-}H}^{as}$) and Amide II (the combination band of 60% N-H bending vibration and 40% C-N stretching vibration) of TA in the region of 1950-1990 nm has been chosen, because this $\nu_{N\text{-}H}^{as}$+Amide II combination band has a larger molar absorption coefficient compared with the other bands, and is not interfered by other overtone or combination bands.

The $\nu_{N\text{-}H}$+Amide II combination band of TA:TMU in $CCl_4$ as a function of temperature and concentration is shown in Figure 1 and Figure 2, respectively. The absorption spectrum of TA(4 mM)/TMU(24 mM)/$CCl_4$ as a function of temperature are shown in Figure 1(a). The appearance of an isosbestic point indicates an equilibrium of only two species, monomeric and hydrogen-bonded TA. The hydrogen-bonded complex should be the 1:1 TA:TMU complex. In the temperature range between 5 °C and 45 °C and at this concentration ratio, the formation of an 1:2 hydrogen-bonded complex was not observed. An intense peak at 1965 nm (5089 $cm^{-1}$) and a shoulder at 1971 nm (5076 $cm^{-1}$) were assigned to monomeric TA and the hydrogen-bonded TA, respectively. The spectrum was resolved into its two Gaussian-Lorentzian product components, each of which was defined by the following equation,[13]

$$A(\nu)_{L\text{-}G} = X_1[1 + X_3^2(\nu - X_2)^2]^{-1} \cdot \exp[-X_4^2(\nu - X_2)^2] \quad (1)$$

where $A(\nu)$ is the absorbance at frequency $\nu$, $X_1$ is the peak height at $\nu_{max}$, $X_2$ is the frequency at band center ($\nu_{max}$), $X_3$ is $1/b_L$ ($b_L$ is the Lorentzian full width at half maximum), and $X_4$ is $\sqrt{\ln 2}/b_G$ ($b_G$ is the Gaussian full width at half maximum). A modified simplex search algorithm was used for curve fitting. The program terminates its iteration when chi square is less than $1\times10^{-9}$.

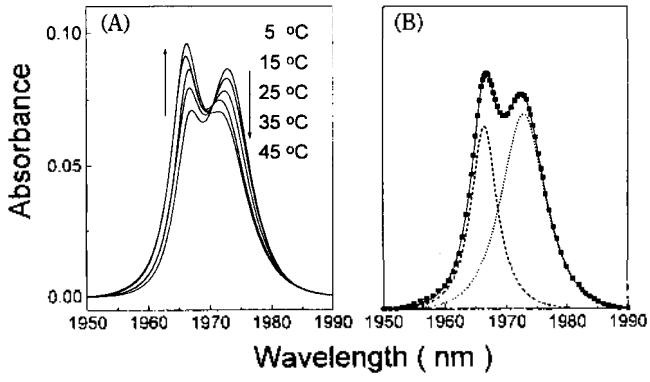


**Figure 1.** (A) The $\nu_{N\text{-}H}^{as}$+Amide II combination band of TA(4 mM)/TMU(24 mM)/$CCl_4$ as a function of temperature. As the temperature increases, the intensity of the band at 1965 nm increases while the intensity of the shoulder at 1971 nm decreases. (B) The resolved $\nu_{N\text{-}H}^{as}$+Amide II combination band at 25 °C. Filled squares (■), dashes line (--), and dots (···) respresent the measured absorption spectrum, resolved band of monomeric TA, and resolved band of hydrogen bonded TA, respectively. The full line is the sum of resolved monomeric and hydrogen bonded TA bands.

The deconvoluted spectrum of TA(4 mM)/TMU(24 mM)/$CCl_4$ at 25 °C are shown in Figure 1(b). As the temperature increases, the area of the monomeric TA band increases, but that of the 1:1 complex decreases. It implies that the equilibrium constant for hydrogen-bond formation becomes smaller and the reaction is exothermic. According to the previous study, the spectrum of TA/$CCl_4$ shows a band at the position of the hydrogen bonded-TA band, which has not been identified yet.[13] The area of this unknown band is 22.7% of total monomer band area. The area of hydrogen bonded TA band was corrected by subtracting the area of the unknown band.

The equilibrium for the hydrogen bond formation and its equilibrium constant K are represented by the following equations:

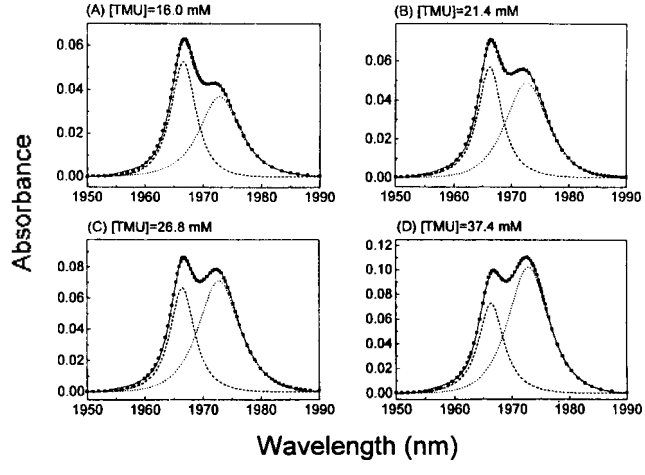


**Figure 2.** The resolved $\nu_{N\text{-}H}^{as}$+Amide II combination band of TA for 1:6 TA:TMU in $CCl_4$ solutions at 25 °C. TMU concentrations are (A) 16.0 mM, (B) 21.4 mM, (C) 26.8 mM, and (D) 37.4 mM TA, respectively.

$$TA + \rightleftarrows TMUTA\cdots TMU$$

$$K = \frac{[TA\cdots TMU]}{[TA]_{free}[TMU]_{free}}$$

where [TA···TMU] is the concentration of the hydrogen-bonded TA, $[TA]_{free}$ is the concentration of monomeric TA, and $[TMU]_{free}$ is the concentration of the free proton acceptor. The ratio of [TA···TMU] to [TA]free is directly obtained from the area of the two resolved bands, and the linear fit for the [TA···TMU]/[TA···TMU] *vs.* $[TMU]_{free}$ plot yields the equilibrium constant. Figure 2 shows the deconvoluted spectrum as a function of TA concentration at 25 °C, showing that the area of 1 : 1 complex band increases with increasing TA concentration. The mole ratio is enough small so that the 1 : 2 formation is negligible.

The value of the equilibrium constant determined at various temperature has been plotted as ln *K vs.* 1/*T* (van't Hoff plot) as shown in Figure 3. The $\Delta H^\circ$ was calculated from the slope of a least-square fitted line for the data points. The equilibrium constants for TMU and DMDPU as a function of temperature are in Table 1. The value of $\Delta H^\circ$ and $\Delta S^\circ$ are in the same table. The $\Delta H^\circ$ for TMU and DMDPU are −23.0 kJ/mol and −19.8 kJ/mol, respectively. The equilibrium constants, $\Delta H^\circ$, and $\Delta S^\circ$ of DMA and DMF are also listed in Table 1.

Thermodynamic parameter $\Delta H^\circ$ listed in Table 1 indicates that the nature of substituents on either side of amide group influences the strength of the hydrogen bond. To a large extent, the chemical properties of amides are determined by resonance structure. When the methyl group is replaced by $N(CH_3)_2$ which is more electron donating group than the methyl group, the increased electron density of oxygen atom is expected, which leads an increase of basicity. This explains why $-\Delta H^\circ$ of TMU is larger than that of DMA. When methyl group of TMU is replaced by phenyl group which is more electron withdrawing group, the decreased electron density on oxygen leads to a decrease in the basicity of amide, which explain our results of DMDPU. Thus the inductive effect of substituents on the oxygen charge density is directly related to the intrinsic strength of hydrogen bonding.

Le Questel *et al.* reported the basicity of secondary and tertiary amides, ureas, and lactams for the formation of 4-fluorophenol-base hydrogen-bonded complex using IR spectroscopy.[14] They observed that TMU is not more basic than DMA. Therefore, in order to confirm the electron-donating effect of $N(CH_3)_2$, we have carried out *ab intio* calculations as follows.

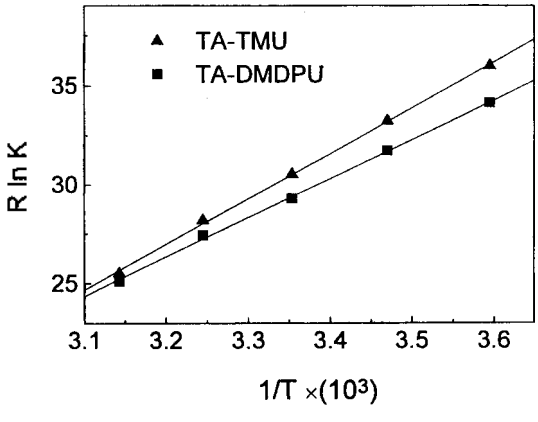


**Figure 3.** The van't Hoff plot for the TA:TMU and TA:DMDPU 1 : 1 complex formaion.

**Table 1.** Thermodynamic parameters for the formation of TA-urea derivative and TA-amide hydrogen-bonded complexes in $CCl_4$ solution

| | K ($M^{-1}$) | | | | | $-\Delta H^\circ$ | $-\Delta S^\circ$ |
|---|---|---|---|---|---|---|---|
| | 5 °C | 15 °C | 25 °C | 35 °C | 45 °C | (kJ/mol) | (J/mol·K) |
| TMU | 76.0 | 54.6 | 39.4 | 29.7 | 21.5 | 23.0(±0.4) | 46.8(±1.4) |
| DMDPU | 60.9 | 45.6 | 34.0 | 27.1 | 20.5 | 19.8(±0.4) | 37.2(±1.3) |
| DMA[a] | 75.6 | 65.4 | 51.3 | 42.1 | 35.3 | 14.4(±1.7) | 15.5(±1.5) |
| DMF[b] | 84.7 | 69.8 | 58.3 | 48.0 | 40.8 | 13.4(±0.2) | 10.6(±0.7) |

[a]Ref. 13(c), [b]Ref. 13(a)

***Ab intio* quantum mechanical calculation.** All the structures were optimized at the restricted Hartree-Fock level using the standard split-valence-shell basis sets. And the vibration frequencies were calculated to obtain the zero point vibrational energies (*ZPVE*) for the corrections of the thermodynamic data.

The proton affinity (PA) of a molecule can be defined as the enthalpy change, $-\Delta H$, at 298.15 K for the process $B(g)+H^+(g) \rightarrow BH^+(g)$, where B is the base. The PA is a measure of the intrinsic basicity of the base toward the proton. From molecular orbital calculations, the proton affinity is equated as follows:

$$\Delta E = E(products) - E(reactants)$$
$$= \Delta E^\circ_{elec} + \Delta ZPVE + \Delta E_{vib}(298.15\ K) - (3/2)RT \quad (2)$$

$$PA(B) = -\Delta H_{298.15}$$
$$= -\Delta E^\circ_{elec} - \Delta ZPVE - \Delta E_{vib}(298.15\ K) + (5/2)RT \quad (3)$$

where $\Delta ZPVE$ is the zero-point vibrational energy change, $\Delta E_{vib}$(298.15 K) is the vibration energy change at 298.15 K, and $E^\circ_{elec}$ is the electronic energy change.

The geometric parameters of optimized TMU are listed in Table 2. The geometry optimization has been carried out for DMA and DMF as well. The protonated TMU, DMA, and DMF are optimized, and their optimized geometry parameters are also presented in Table 2. The optimized molecular geometries of DMA and DMF are both planar, but TMU has a pyramidal configuration about the nitrogen atoms.

The structures of urea and its derivatives were believed to be planar because the C-N bond has a partial double-bond character. Experimental X-ray and neutron diffraction data show a planar structure for the urea molecule in the crystal structure.[15] Recently, the crystal structure of the complex of *N,N'*-bis(4,4'-difluoro-2-biphenyl)urea with TMU has been determined by single crystal X-ray diffraction, showing that the nearest environment for the N atoms is planar.[16] The structure of TMU in $CCl_4$ solution has been identified to be planar by NMR spectroscpy.[17] However, the microwave spectrum of the urea in gas phase indicates a nonplanar structure.[18] Recent *ab initio* calculation shows that the amino group of the urea and its derivatives in gas phase have a pyramidal structure.[19,20] In this work, we have confirmed a pyramidal configuration about the nitrogen atom for the fully optimized TMU in gas phase.

**Table 2.** Calculated geometrical parameters for TMU, DMA, DMF and protonated TMU, DMA, DMF

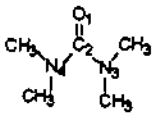
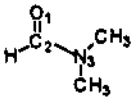
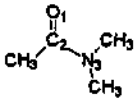

| | HF/3- | HF/6-31G(d) | HF/3-21G | HF/6-31G(d) |
|---|---|---|---|---|
| | TMU | | Protonated TMU | |
| Bond length (Å) | | | | |
| C2-O1 | 1.222 | 1.202 | 1.335 | 1.309 |
| C2-N3 | 1.378 | 1.380 | 1.313 | 1.317 |
| N3-C5 | 1.463 | 1.451 | 1.488 | 1.473 |
| N4-C6 | 1.466 | 1.453 | 1.488 | 1.473 |
| Bond angle (deg) | | | | |
| O1C2N3 | 122.1 | 122.0 | 111.8 | 112.2 |
| C2N3C5 | 117.1 | 115.5 | 126.4 | 126.2 |
| C2N3C6 | 122.2 | 120.7 | 117.0 | 116.9 |
| Dipole moment (D) | 3.672 | 3.394 | 1.921 | 1.700 |
| | DMA | | Protonated DMA | |
| Bond length (Å) | | | | |
| C2-O1 | 1.222 | 1.204 | 1.323 | 1.294 |
| C2-N3 | 1.358 | 1.356 | 1.280 | 1.283 |
| N3-N3 | 1.463 | 1.452 | 1.495 | 1.479 |
| Bond angle (deg) | | | | |
| O1C2N3 | 121.0 | 121.3 | 115.5 | 116.3 |
| C2N3C5 | 124.1 | 123.8 | 122.3 | 121.9 |
| C2N3C6 | 115.8 | 116.0 | 119.0 | 119.0 |
| Dipole moment (D) | 4.113 | 4.052 | 2.128 | 1.910 |
| | DMF | | Protonated DMF | |
| Bond length (Å) | | | | |
| C2-O1 | 1.216 | 1.197 | 1.311 | 1.288 |
| C2-N3 | 1.350 | 1.356 | 1.271 | 1.272 |
| N3-N3 | 1.463 | 1.452 | 1.502 | 1.484 |
| Bond angle (deg) | | | | |
| O1C2N3 | 124.6 | 125.0 | 119.2 | 120.3 |
| C2N3C5 | 120.4 | 120.1 | 120.2 | 119.9 |
| C2N3C6 | 117.6 | 117.8 | 119.7 | 119.9 |
| Dipole moment (D) | 4.292 | 4.231 | 2.808 | 2.620 |

Recent studies show that when the oxygen of amide group rather than the nitrogen atom is protonated, the protonated amides and urea become more stable.[21,22] Therefore, the geometry of protonated molecule has been optimized for the oxygen site protonation, showing that the heavy atom skeletons of protonated amides and TMU lie close to the plane. As protonated, the C-O bond lengths are increased and the C-N bond lengths are decreased. In the case of TMU, the C-O bond is lengthened by 11.3% and 10.5% and the C-N bond is shortened by 6.5% and 6.3%, respectively, with HF/3-21G and HF/6-31G(d) basis sets. As protonated in DMA, the C-O bond lengths are increased by 10.1% and 9.5%, and the C-N bond lengths are decreased by 7.8% and 7.3%, respectively, with HF/3-21G and HF/6-31G(d) basis sets. In the case of DMF, the C-O bond is lengthened by 9.5% and 9.1% and the C-N bond is shortened by 7.9% and 7.4%, respectively, with HF/3-21G and HF/6-31G(d) basis sets. The structural parameters of DMA and DMF are found to be consistent with those of Wiberg *et al.*[23] The calculations show that as protonated, the bond length of C-O and C-N are increased and decreased, respectively, following the order of TMU>DMA>DMF.

The PA of TMU, DMA, and DMF at HF/3-21G and HF/6-31G(d) levels are reported in Table 3, showing that the PA increases in the order of TMU>DMA>DMF, which is consistent with our experimental result in $CCl_4$ solution. One might expect to correlate the basicity of amides with the oxygen charge; the greater the electron density on the oxygen atom, the greater its basicity. We obtain the Mullikan atomic charge of oxygen atom as −0.626, −0.619, and −0.578 for optimized TMU, DMA, and DMF, respectively. There is a good correspondence between charge carried by the oxygen and the gas phase basicity. It is evident that the electrostatic interaction is dominant in the strength of hydrogen bonds. We conclude that the *ab initio* PA calculations in gas phase can serve as a basis for analyzing the factors which influence the hydrogen bonding formation in $CCl_4$ solution.

In summary, the hydrogen-bonding interactions between thioacetamide (TA) and urea derivatives such as tetramethylurea (TMU) and dimethyldiphenylurea (DMDPU) in $CCl_4$ solution have been studied experimentally using near-infrared absorption spectroscopy. Thermodynamic parameters for the interactions between TA and urea derivatives are determined by analyzing the $\nu^{as}_{N\text{-}H}$+Amide II combination band of TA at 1970 nm. The $\Delta H^\circ$ values are measured to be −23.0 kJ/mol and −19.8 kJ/mol for TMU and DMDPU, respectively. *Ab initio* molecular orbital calculations for the proton affinity of TMU, *N,N*-dimethylformamide (DMF), and *N,N*-dimethylacetamide (DMA) in gas phase have been carried out using HF/3-21G and HF/6-31G(d) basis sets, showing that the proton affinity is in the order of TMU>

**Table 3.** Calculated zero-point vibrational energy (*ZPVE*), electronic energy ($E_{elec}$) and proton affinity (PA) for TMU, DMA, and DMF with protonated species at HF/3-21G and HF/6-31G(d) levels (1 hartree=2625 kJ/mol)

| | HF/3-21G | | | HF/6-31G(d) | | |
|---|---|---|---|---|---|---|
| | *ZPVE* (hartree)[a] | $E_{elec}$ (hartree) | *PA* (kcal/mol) | *ZPVE* (hartree)[a] | $E_{elec}$ (hartree) | *PA* (kcal/mol) |
| TMU | 0.189074 | −377.601941 | 336.2513 | 0.189830 | −379.708160 | 328.2839 |
| Protonated TMU | 0.203162 | −378.350015 | | 0.204209 | −380.445015 | |
| TMA | 0.139599 | −284.434546 | 220.1662 | 0.139806 | −286.026634 | 213.9532 |
| Protonated DMA | 0.152939 | −284.808470 | | 0.153901 | −286.390906 | |
| DMF | 0.109519 | −245.609542 | 212.3405 | 0.109831 | −246.986615 | 205.9155 |
| Protonated DMF | 0.123144 | −245.971444 | | 0.124286 | −247.339805 | |

[a]HF/3-21G and HF/6-31G(d) harmonic vibrational frequencies scaled by 0.891.

DMA > DMF. We found that the proton affinity in gas phase and the hydrogen bonding ability in $CCl_4$ solutions are correlated well with each other.

**Acknowledgment.** This work was supported by the Basic Science Research Institute Program funds(BSRI-96-3405, BSRI-96-3432).

## References

1. Ellerton, H. D.; Dunlop, P. *J. Phys. Chem.* **1966,** *70*, 1831.
2. Wetlaufer, D. B.; Malik, S. K.; Stoller, L.; Coffin, R. I. *J. Am. Chem. Soc.* **1964,** *86*, 508.
3. Brandts, J. F.; Hunt, L. J. *J. Am. Chem. Soc.* **1967,** *89*, 4826.
4. Frank, F. S.; Franks, F. *J. Chem. Phys.* **1968,** *48*, 4746.
5. (a) Kreschek, G. C.; Schergaga, H. A. *J. Chem. Phys.* **1965,** *69*, 1704. (b) Stokes, R. H. *Aust. J. Chem.* **1967,** *20*, 2087.
6. (a) Kuharski, R. A.; Rossky, P. J. *J. Am. Chem. Soc.* **1984,** *106*, 5736. (b) Kuharski, R. A.; Rossky, P. J. *ibid.* **1984,** *106*, 5794.
7. (a) Tanaka, H.; Touhara, H.; Nakanishi, K.; Watanabe, N. *J. Chem. Phys.* **1984,** *80*, 5170. (b) Tanaka, H.; Nakanishi, K.; Touhara, H. *ibid.* **1985,** *82*, 5184.
8. (a) Cristinziano, P.; Lelj, F.; Amodeo, P.; Barone, V. *Chem. Phys. Lett.* **1987,** *140*, 401. (b) Cristinziano, P.; Lelj, F.; Amodeo, P.; Barone, V. *J. Chem. Soc., Faraday Trans. I* **1989,** *85*, 621.
9. Finney, J. I.; Turner, J. *Electrochim, Acta* **1988,** *9*, 1183.
10. Barone, G.; Rizzo, E.; Vitagliano, V. *J. Phys. Chem.* **1970,** *74*(10), 2230.
11. Subramanian, S.; Balasubramanian, D.; Ahluwalia, J. C. *J. Phys. Chem.* **1969,** *75*(6), 815.
12. Jancsó, G.; Cser, L.; Grósz T.; Ostanevich, Yu. M. *Pure & Appl. Chem.* **1994,** *66*(40), 515.
13. (a) Choi, Y. S.; Huh, Y. D.; Bonner, O. D. *Spectrochimica Acta A* **1985,** *41*, 1127 (1985). (b) Choi, Y. S.; Kim, J.; Park, J.; Yu, J.; Yoon, C. J. *Spectrochimica Acta A* **1985,** *52*, 1127. (c) Lee, K. B.; Kim, B. C.; Bonner, O. D.; Choi, Y. S. *J. Korean Chem. Soc.* **1986,** *30*, 510.
14. Le Questel, J. Y.; Laurence, C.; Lachkar, A.; Helbert, H.; Berthelot, M. *J. Chem. Soc., Perkin Trans. 2* **1992,** 2091.
15. Caron, A.; Donohue, J. *Acta Crystallgr. Sect. B* **1969,** *25*, 404.
16. Wozniak, K.; Wawer, I.; Ströhl, D. *J. Phys. Chem.* **1995,** *99*, 8888.
17. Nyuist, R. A.; Streck, R.; Jeschek, G. *J. Mol. Struc.* **1996,** *377*, 113.
18. Brown, R. D.; Godfrey, P. D.; Storey, J. *J. Mol. Spectrosc.* **1975,** *58*, 445.
19. Meier, R. J.; Coussens, B. *J. Mol. Struc. (Theochem)* **1992,** *253*, 25.
20. Töth, K.; Bopp, B.; Peräkylä, M.; Pakkanen, T. A.; Jancsó, G. *J. Mol. Struct. (Theochem)* **1994,** *312*, 93.
21. Ou, M. C.; Chu, S. Y. *J. Phys. Chem.* **1995,** *99*, 556.
22. Lin, C. K.; Chen, S. Y.; Lien, M. H. *J. Phys. Chem.* **1995,** *99*, 1454.
23. Wiberg, K. B.; Rablen, P. R.; Rush, D. J.; Keith, T. A. *J. Am. Chem. Soc.* **1995,** *117*, 4261.